Structure of an Accurate ab Initio Model of the Aqueous Cl^- Ion at High Temperatures

Haitao Dong,[†] Wenbin Liu,[‡] Douglas Doren, and Robert Wood*

Department of Chemistry and Biochemistry, University of Delaware, Newark, Delaware 19716

Received: May 9, 2006; In Final Form: July 7, 2006

The structure of an accurate ab initio model of aqueous chloride ion was calculated at two high-temperature state points (573 K, 0.725 g/cm^3 and 723 K, 0.0098 g/cm^3) by a two-step procedure. First, the structure of an approximate model was calculated from a molecular dynamics simulation of the model. Then the difference between the structure of the ab initio model and the approximate model was calculated by non-Boltzmann weighting of a sample of configurations taken from the approximate model simulation. Radial distribution functions, average coordination numbers, the distribution of coordination numbers, an analysis of orientations of water in the first coordination shell, and the free energy of hydration of the chloride ion are reported for both state points. The most common water structure has one hydrogen close to the chloride ion and one pointing away (46% at 573 K and 57% at 723 K). Waters in the first coordination shell that are not strongly bound to the chloride ions are common. Several variations of the method were tested. Models in which the water−water interaction is calculated with ab initio methods predict only a slightly different structure than models in which water−water interactions are determined from the approximate models. Similarly, using the approximate model for solute−water interactions when the water is far from the chloride ion did not affect the results. Uncertainties due to the limited sample of configurations are estimated and found to be small. The results are in qualitative agreement with X-ray and neutron diffraction experiments and with simulations of approximate models.

1. Introduction

This paper is part of a series developing and exploiting computational methods for predicting the free energy and structure of high-temperature aqueous electrolyte solutions.[1−6] Fundamental studies of thermodynamic properties and structures of water−salt systems under extreme conditions have important implications for industrial and natural chemical processes such as solid deposition, metal corrosion in steam cycles, solvent extraction, and hydrothermal ore formation.[7−10] In this paper, we use a new method to calculate the structure of the first hydration sphere of an aqueous chloride ion at two high-temperature state points, one at high density (0.725 g/cm^3, 573 K) and the other at low density (0.0098 g/cm^3, 723 K). These two points were chosen as representative of the environments found for Cl^-(aq) in hydrothermal solutions and steam cycles in electric power plants.

Experimental measurements of the structure of water around an aqueous Cl^- ion are very difficult even at ambient conditions. The older literature has been reviewed by Ohtaki and Radnai.[11] The best current technique is neutron diffraction with isotopic substitution, but this requires the use of concentrated aqueous solutions (usually >1 mol/kg), which may not have the same structure as dilute solutions. There are very few results even for moderately high-temperature aqueous solutions of Cl^- because of experimental difficulties, and low water densities cannot be studied because of low solubility.

In contrast to experimental methods, molecular dynamics or Monte Carlo simulations with models of the interactions between Cl^- and water are not limited in temperature and pressure and give far more detailed information about the structure. However, the reliability of the results is limited by the accuracy of the model for the interaction energies between the molecules. A large number of papers report studies with molecular mechanics models for the interactions (for instance Lennard-Jones plus charge models). These models almost always give the same qualitative conclusions, which are presumably correct. Estimates of the difference between the properties of the calculated model and the "real world" are almost completely missing from the discussion, so no quantitative tests of the model information are available. A recent comparison of models for Na^+ and Cl^- shows important quantitative differences.[12] For some other recent examples of this type of calculation for aqueous Cl^-, see Konishan et al.,[13] Kubo et al.,[14] and Chialvo and Simonson.[15] It is also possible to do molecular dynamics calculations with quantum mechanical models, but the present available computing power limits most of these calculations to DFT models with somewhat limited plane-wave basis sets, small unit cells, and short simulation times (for further discussion see Balbuena and Seminario[16]). Examples of such calculations for chloride ions have included solvation in clusters of water[17−20] and a periodic model with 64 water molecules in the unit cell.[21] Simulations of aqueous Cl^- have also been done with a variety of hybrid QM/MM models, but none are at high temperatures. The QM/MM studies to date have included models of room-temperature liquid water treated with self-consistent field methods (AM1, Hartree−Fock, or DFT),[19−26] and water clusters in the zero temperature limit treated with Hartree−Fock and MP2.[27,28]

The present approach allows calculation of configurational averages for a QM/MM model with higher-level electronic structure methods than previously possible. The basic idea behind this method is simple. Simulations with an approximate

* Corresponding author. E-mail: rwood@udel.edu.
[†] Current address: Department of Chemistry, Oregon State University, Corvallis, Oregon.
[‡] Current address: Quest Pharmaceutical Services, Newark, Deleware.

10.1021/jp0628333 CCC: $33.50
Published on Web 08/31/2006

potential, U^A, are used to generate an ensemble of thermally accessible configurations. Calculations of the ab initio interaction potential, U^Q, are needed only for a sample of statistically independent configurations taken from the simulation with U^A. Free energy perturbation is used to calculate the difference in free energy of the two models.[1] Similarly, non-Boltzmann weighting can be used to calculate the difference between the structural properties of the ab initio and approximate models.[5] An important aspect of this method is that the approximate potential is used to generate a distribution of configurations, while the ab initio method determines the energy and weight of each configuration in the average. Standard statistical methods can be used to determine whether the configurations sampled with U^A are representative of the configurations that are important for U^Q. As long as the configuration sampling is adequate, the quality of the effective potential does not determine the predictions of the method.

In practice, this approach allows calculations of free energies and structures that are several orders of magnitude faster than full ab initio simulations at the same level because ab initio energies are needed only for a small number of configurations. Other researchers have used similar methods to facilitate the determination of the properties of quantum models.[29−37] We achieve an additional savings in computational effort by separating the interaction energies into pair and multibody interactions to reduce the computational cost of the calculations.[1] This is very effective because the multibody terms can be accurately calculated with density functional theory (DFT) instead of the more time-consuming second-order Moller−Plesset (MP2) perturbation calculations that are needed for accurate pair interactions.

In this paper, we report the structure and radial distribution function (RDF) of aqueous chloride ion at two state points. The two great advantages of this method are that high-level quantum mechanical methods can be used and the differences between the models and the "real world" can be estimated. This model gives a structure of unprecedented accuracy that we believe is close to the structure of real, high-temperature aqueous solutions of chloride ion.

In Section 2, we present the theoretical basis and computational details of our calculations of free energies, structures, and their uncertainties. In Section 3, we present the results of our calculations, and Section 4 gives a comparison of our results with the previous experiments and simulations, together with a discussion of the uncertainties introduced by the limitations of the present method.

2. Theoretical Basis

2.1 The ABC-FEP Method for Free Energies. Consider the high-temperature hydration of Cl^-, which is characterized by the quantum mechanical potential U^Q, or the approximate potential U^A. The free energy difference ΔG between the two models can be calculated as

$$\Delta G(\mathrm{A} \rightarrow \mathrm{Q}) = G^{\mathrm{Q}} - G^{\mathrm{A}} = -k_{\mathrm{B}}T \ln(\langle \exp(-\Delta U/k_{\mathrm{B}}T)\rangle_{\mathrm{A}}) \quad (1)$$

where $\Delta U = U^Q - U^A$ and $\langle\ \rangle_A$ implies an average taken over configurations generated by the simulation with the approximate potential. We have previously applied eq 1 to calculations of hydration free energies of an ab initio model of Na^+ and Cl^- in supercritical water from configurations of a simulation of an approximate model.[3,4,6] We have shown[3] that 100 independent configurations are enough to give a hydration free energy within 7 kJ/mol of the experimental values at 573 K and 0.725 g/cm^3.

2.2. Non-Boltzmann Weighting for RDF and Coordination Numbers. Equation 1 can be thought of as non-Boltzmann weighting to calculate the ratio of partition functions that in turn is used to calculate the free energy difference.[5] More generally, the average of a mechanical variable, M, of the quantum mechanical potential can be calculated from a simulation of the approximate model using non-Boltzmann weighting[5,38,39]

$$\langle M\rangle_{\mathrm{Q}} = \frac{\langle M \exp(-\Delta U/k_{\mathrm{B}}T)\rangle_{\mathrm{A}}}{\langle \exp(-\Delta U/k_{\mathrm{B}}T)\rangle_{\mathrm{A}}} = \sum_i^{N_{\mathrm{conf}}} M_i W_i \quad (2)$$

where $W_i = \exp(-\Delta U_i/k_BT)/\sum_i^{N_{conf}} \exp(-\Delta U_i/k_BT)$ acts as a non-Boltzmann weighting factor and N_{conf} is the number of independent configurations studied. The difference between quantum and approximate models can be calculated as

$$\Delta M = \langle M\rangle_{\mathrm{Q}} - \langle M\rangle_{\mathrm{A}} = \sum_i^{N_{\mathrm{conf}}} M_i(W_i - 1) \quad (3)$$

If N_{ij} is the number of oxygen atoms in the jth bin (with R_{Cl-O} between $r_j - {}^1/_2\ dr$ and $r_j + {}^1/_2\ dr$) of the ith configuration of the approximate model, then the radial distribution function at r_i in the approximate model, $g^A_{Cl-O}(r_j)$, is calculated using

$$g^{\mathrm{A}}_{\mathrm{Cl-O}}(r_j) = \sum_i^{N_{\mathrm{conf}}} N_{ij}/(V_j\rho_0 N_{\mathrm{conf}}) \quad (4)$$

where V_j is the volume of the jth bin, $V_j = (4/3)\pi((r_j + ({}^1/_2)\ dr)^3 - (r_j - ({}^1/_2)\ dr)^3)$, and ρ_0 is the bulk number density of oxygen atoms.[5] The differences between the RDFs for the Q and A models is calculated using

$$\Delta g_{\mathrm{Cl-O}}(r_j) = \sum_i^{N_{\mathrm{conf}}} N_{ij}(W_i - 1)/(V_j\rho_0 N_{\mathrm{conf}}) \quad (5)$$

If we define the running coordination number, $N_O[r]$, as the number of oxygen atoms with the Cl^- to O distance, R_{Cl-O}, less than r in the ith configuration, then the average running coordination number of O around Cl^- for the approximate model is

$$N^{\mathrm{A}}_{\mathrm{O}}[r] = \sum_i^{N_{\mathrm{conf}}} N_{\mathrm{O}}[r, i]/N_{\mathrm{conf}} \quad (6)$$

and for the quantum model it is

$$N^{Q}_{O}[r] = \sum_i^{N_{\mathrm{conf}}} N_{\mathrm{O}}[r, i]W_i/N_{\mathrm{conf}} \quad (7)$$

If we define the first coordination sphere as containing all those water molecules with oxygens that are inside R_{cut}, then the average coordination numbers are $N^A_O[R_{cut}]$ and $N^Q_O[R_{cut}]$ for the two models. The probabilities of a configuration having $N_O[R_{cut}] = n$ in the two models are

$$P^{\mathrm{A}}_{\mathrm{O}}[R_{\mathrm{cut}}, n] = \sum_i^{N_{\mathrm{conf}}} \delta(N_{\mathrm{O}}[R_{\mathrm{cut}}, i] - n)/N_{\mathrm{conf}} \quad (8)$$

and

$$P_{\mathrm{O}}^{\mathrm{Q}}[R_{\mathrm{cut}}, n] = \sum_{i}^{N_{\mathrm{conf}}} \delta(N_{\mathrm{O}}[R_{\mathrm{cut}}, i] - n) W_i / N_{\mathrm{conf}} \qquad (9)$$

where $\delta(N_{\mathrm{O}}[R_{\mathrm{cut}}, i] - n)$ is 1 only when $N_{\mathrm{O}}[R_{\mathrm{cut}}, i] = n$. Equations 4−9 can be applied to hydrogen atoms as well.

In the ABC-FEP method of calculating $\Delta_h G$ of hydration, only the Cl^-−water interactions can be changed to quantum interactions because changes in the water−water interactions are not part of the free energy of hydration of Cl^-. Thus, $\Delta_h G$ calculated this way is the free energy of a chloride ion with quantum Cl^-−water interactions (both pair and multibody) and approximate water−water interactions. However, when calculating a mechanical variable like RDF or coordination number, we can in principle change all classical interactions, including those between water molecules, to quantum interactions and get the mechanical variable for this model. In practice, including ΔU_{ww} increases the noise of our results as discussed in the Results section. To further reduce the computational demand of this method, we only calculate the ab initio solute−solvent interactions between Cl^- and the n_{Clw} nearest water molecules and ab initio solvent−solvent interactions between the n_{ww} nearest water molecules. This approximation depends on having an approximate model that accurately reproduces the long-range ion−water interactions.

2.3. Pair and Multibody Interactions. The interaction energy $U_{\mathrm{Clw}}^{\mathrm{Q}}$ can be considered as a sum of the pairwise and the multibody interaction energies of the solute Cl^- with the water molecules[1]

$$U_{\mathrm{Clw}}^{\mathrm{Q}} = U_{\mathrm{Clw,pair}}^{\mathrm{Q}}[n_{\mathrm{Clw}}] + U_{\mathrm{Clw,multi}}^{\mathrm{Q}}[m_{\mathrm{Clw}}] \qquad (10)$$

where m_{Clw} is the number of water molecules included in the multibody energy. The pairwise energy in eq 10 is simply a sum of n_{Clw} water pair energies

$$U_{\mathrm{Clw,pair}}^{\mathrm{Q}} = \sum_{i}^{n_{\mathrm{Clw}}} U_{\mathrm{Clw}}^{\mathrm{Q}}[\mathrm{Cl{-}water}(i)] \qquad (11)$$

and the multibody energy is the difference between the total interaction energy and the pairwise energies with the m_{Clw} water molecules. Note that m_{Clw} can be much less than n_{Clw} without reducing accuracy because multibody interactions are relatively short-ranged. This separation into pair and multibody interaction energies leads to substantial savings in computational effort because different levels of theories can be used for pair and multibody energies.[40] We find that, while the pair energies must be determined with the MP2 level of theory, the multibody interactions can be determined with the same level of accuracy with less demanding ab initio methods, e.g., density functional theory.[3]

In a similar way, we can divide the water−water interaction energies into pairwise and multibody contributions: $U_{\mathrm{ww,pair}}^{\mathrm{Q}}(n_{\mathrm{ww}})$ for the sum of the pairwise interactions of the nearest n_{ww} waters and $U_{\mathrm{ww,multi}}^{\mathrm{Q}}(m_{\mathrm{ww}})$ for the multibody interactions among the nearest m_{ww} water molecules.

2.4. Computational Details. Classical molecular dynamics simulations were performed for Cl^- in supercritical water at two state points, 723 K and 0.0098 g/cm^3 and 573 K and 0.725 g/cm^3. An MD simulation package, DL_POLY, with modifications to incorporate the TIP4P−FQ water model potential was used.[41,42] The approximate model of Liu et al. was used for the chloride ion interactions with water (van der Waals exponents of 9 and 6 plus Coulombic interaction).[3] Each of the simulation boxes was first prepared with one chloride ion and 200 water molecules at the target temperature and pressure with the periodic boundary conditions and Ewald sums (with neutralizing background charge) for the electrostatic forces. A van der Waals cutoff of 35 Å for the low-density and 8.5 Å for the high-density state point was used. The *NPT* simulation was run with a step size of 0.5 fs for 50 ps to equilibrate the system, and then 500 independent configurations were collected at intervals of 25 ps at low density and 5 ps at high density. Velocity autocorrelation functions and the frequency of coordination number changes showed that the configurations were independent.

All the ab initio calculations were performed with the *Gaussian03* package.[43] The pairwise energies were calculated at the MP2/aug-cc-pVDZ level, while B3LYP/aug-cc-pVDZ was used for the multibody interactions. All the ab initio interaction energies were corrected for the basis set superposition error (BSSE) using the standard counterpoise method.[44] Liu et al. have shown that $n_{\mathrm{Clw}} = 15$ and $m_{\mathrm{Clw}} = 7$ was adequate for the low-density state point and $n_{\mathrm{Clw}} = 60$ and $m_{\mathrm{Clw}} = 7$ was adequate for the high-density state point.[3] The approximate model energies of the configurations with the same [n, m] combinations were also needed for calculating $\Delta U = U^{\mathrm{Q}} - U^{\mathrm{A}}$.

2.5 Estimation of Uncertainties by Bootstrap Resampling. We have estimated uncertainties of our results using bootstrap resampling. The details of the procedure are given by Efron.[45] A brief heuristic explanation is as follows. Given a very large sample of some experimental results (for instance ΔU) that can be used to calculate a desired quantity (for instance, $\Delta_h G$ using eq 1), it is very easy to estimate the uncertainty of using a limited sample (say 500). One repeatedly selects at random 500 examples (with duplication allowed) and calculates the standard deviation of the results of this repeated sampling. Because in our present case we only have 500 samples, our best estimate of the error of taking only 500 samples is obtained by resampling (with duplication allowed) our sample of 500. Our experience with this method is that the uncertainties it yields are very reasonable. In the present paper, we report standard deviations, σ, of the resampled results so that 95% confidence limits would be about twice as large.

3. Results

3.1. Free Energy. Using ab initio interaction energies for a sample of 500 chloride−water configurations, we calculated $\Delta_h G(\mathrm{A} \rightarrow \mathrm{Q})$ and compared our results to those of Liu et al., which were determined from 80 configurations at 573 K and 50 configurations at 723 K.[3] Liu et al. used a 6-311++G(3df,-3pd) basis set for the pair interactions, the same approximate model and the same values of m and n. The agreement was satisfactory: $\Delta_h G(\mathrm{A} \rightarrow \mathrm{Q}) = -3.5$ and -8.9 kJ/mol at 573 K, respectively, for the present results and those of Liu et al., and -0.2 and 0.6 kJ/mol at 723 K. Our estimated uncertainty due to the quantum methods is about 5 kJ/mol for both calculations. The bootstrap estimated sampling errors with the sample of 500 configurations were small: <1 kJ/mol for all calculations. Extrapolating our results to an infinite number of water molecules ($n_{\mathrm{Clw}} = \infty$) at 573 K decreases the free energy by 1.5 ± 0.5 kJ/mol, so our best estimate is $\Delta_h G(\mathrm{A} \rightarrow \mathrm{Q}) = -5.0$ kJ/mol at 573 K. Extrapolation did not change the result at 723 K.

3.2. Radial Distribution Functions. Extensive calculations of the radial distribution functions and solution structure were made for two quantum models. Both models used $m_{\mathrm{Clw}} = 7$, with $n_{\mathrm{Clw}} = 60$ at 573 K and $n_{\mathrm{Clw}} = 15$ at 723 K. Liu et al. showed this was adequate to obtain converged Cl^-−water

TABLE 1: Number of Atoms within Radius *r* around the Chloride Ion at 573 K and 0.725 g/cm³ for Approximate Model (A), Quantum Models without (Q_1), and with water−water pairwise interactions (Q_{ww})[a]

	Cl−O			Cl−H		
r	N^A	ΔN^{Q1}	ΔN^{Qww}	N^A	ΔN^{Q1}	ΔN^{Qww}
1.904	0	0	0	0.01	0.00(0)	0.00(0)
2.040	0	0	0	0.17	0.01(3)	−0.01(4)
2.176	0	0	0	0.70	0.13(5)	0.13(8)
2.312	0	0	0	1.54	0.11(7)	−0.06(10)
2.448	0	0	0	2.44	0.16(9)	−0.21(22)
2.584	0	0	0	3.26	0.10(7)	−0.21(20)
2.720	0	0	0	3.98	0.04(8)	−0.50(27)
2.856	0.04	0.00(0)	0.01(1)	4.65	−0.05(8)	−0.44(22)
2.992	0.35	0.11(6)	0.01(7)	5.33	−0.13(6)	−0.42(16)
3.128	1.19	0.06(5)	0.22(16)	6.08	−0.24(9)	−0.58(26)
3.264	2.31	0.05(6)	−0.08(6)	7.00	−0.38(11)	−0.88(40)
3.400	3.40	0.01(6)	−0.09(7)	8.20	−0.50(10)	−0.87(25)
3.536	4.35	−0.15(9)	−0.41(16)	9.62	−0.59(10)	−0.64(12)
3.672	5.18	−0.10(8)	−0.29(16)	11.16	−0.57(10)	−0.92(23)
3.808	5.92	−0.19(8)	−0.32(12)	12.69	−0.48(12)	−0.88(32)
3.944	6.61	−0.37(8)	−0.39(8)	14.18	−0.43(16)	−1.13(56)
4.080	7.23	−0.46(8)	−0.58(15)	15.66	−0.32(21)	−1.16(64)
4.216	7.97	−0.23(16)	−0.63(27)	17.17	−0.13(17)	−0.50(32)
4.352	8.67	−0.08(19)	−0.51(24)	18.71	−0.24(18)	−0.11(22)
4.488	9.40	−0.12(16)	−0.37(26)	20.33	−0.22(22)	−0.23(21)
4.624	10.18	−0.05(15)	−0.45(36)	22.06	0.01(26)	0.19(32)
4.760	11.02	−0.11(13)	−0.40(33)	23.90	0.02(30)	0.08(27)
4.896	11.93	−0.27(13)	−0.34(19)	25.88	0.21(36)	0.24(37)
5.032	12.90	−0.24(15)	0.00(28)	28.00	0.13(37)	−0.05(37)
5.168	13.94	0.05(17)	0.20(24)	30.27	0.10(37)	−0.32(46)
5.304	15.07	−0.03(15)	−0.02(21)	32.62	0.01(30)	0.04(34)
5.440	16.29	0.07(16)	0.15(23)	35.13	0.14(28)	0.05(28)
5.576	17.60	0.08(14)	0.09(19)	37.74	0.03(24)	0.06(27)
5.712	19.02	0.01(15)	−0.16(20)	40.50	−0.01(24)	0.29(42)
5.848	20.54	0.06(14)	0.17(17)	43.39	−0.14(29)	0.71(86)
5.984	22.15	0.18(17)	0.65(48)	46.44	−0.35(39)	0.13(67)
6.120	23.83	−0.10(14)	0.20(26)	49.62	−0.34(41)	0.53(89)

[a] $\Delta N^{Qx} = N^{Qx} - N^A$, where Q_x represents Q_1 or Q_{ww}.

TABLE 2: Number of Atoms within Radius *r* around the Chloride Ion at 723 K and 0.0098 g/cm³ for Approximate Model (A), Quantum Models without (Q_1), and with Water−Water Pairwise Interactions (Q_{ww})[a]

	Cl−O			Cl−H		
r	N^A	ΔN^{Q1}	ΔN^{Qww}	N^A	ΔN^{Q1}	ΔN^{Qww}
1.82	0	0	0	0	0	0
1.96	0	0	0	0.09	0.02(1)	0.03(1)
2.10	0	0	0	0.35	0.00(1)	0.02(2)
2.24	0	0	0	0.76	−0.06(2)	−0.04(2)
2.38	0	0	0	1.18	−0.09(2)	−0.07(3)
2.52	0	0	0	1.54	−0.08(2)	−0.06(3)
2.66	0	0	0	1.84	−0.04(2)	−0.03(4)
2.80	0.03	0.01(1)	0.01(1)	2.11	−0.02(3)	0.01(4)
2.94	0.23	0.02(1)	0.02(2)	2.37	0.05(3)	0.08(4)
3.08	0.64	0.02(2)	0.04(2)	2.67	0.10(3)	0.14(4)
3.22	1.14	−0.03(2)	−0.02(2)	3.06	0.16(3)	0.22(5)
3.36	1.57	−0.05(2)	−0.02(3)	3.54	0.18(3)	0.25(5)
3.50	1.90	−0.05(3)	−0.01(3)	4.05	0.17(4)	0.25(6)
3.64	2.14	0.01(2)	0.04(3)	4.52	0.13(4)	0.22(6)
3.78	2.32	0.04(2)	0.07(3)	4.90	0.14(4)	0.25(6)
3.92	2.46	0.07(2)	0.11(3)	5.19	0.17(4)	0.27(6)
4.06	2.58	0.08(2)	0.12(4)	5.43	0.17(5)	0.28(7)
4.20	2.67	0.08(2)	0.11(4)	5.63	0.16(5)	0.28(7)
4.34	2.76	0.09(3)	0.14(4)	5.80	0.18(5)	0.29(8)
4.48	2.83	0.09(3)	0.14(4)	5.96	0.18(5)	0.31(8)
4.62	2.90	0.09(3)	0.14(4)	6.12	0.18(5)	0.32(8)
4.76	2.97	0.09(3)	0.16(4)	6.26	0.18(6)	0.36(8)
4.90	3.04	0.08(3)	0.16(4)	6.40	0.20(6)	0.39(9)
5.04	3.11	0.09(3)	0.16(4)	6.54	0.21(6)	0.42(9)
5.18	3.18	0.10(3)	0.17(4)	6.68	0.21(6)	0.44(9)
5.32	3.24	0.09(3)	0.17(4)	6.81	0.21(6)	0.47(9)
5.46	3.32	0.09(3)	0.20(4)	6.94	0.20(6)	0.48(9)
5.60	3.39	0.09(3)	0.22(5)	7.08	0.20(6)	0.49(9)
5.74	3.46	0.09(3)	0.22(5)	7.20	0.21(6)	0.53(9)
5.88	3.54	0.10(3)	0.23(5)	7.33	0.21(6)	0.52(9)
6.02	3.61	0.10(3)	0.26(5)	7.46	0.20(6)	0.53(10)
6.16	3.68	0.10(3)	0.26(5)	7.58	0.22(7)	0.57(10)

[a] $\Delta N^{Qx} = N^{Qx} - N^A$, where Q_x represents Q_1 or Q_{ww}.

energies. The first quantum model, Q_1, included no corrections for the water−water interactions; i.e., $n_{ww} = 0$ and $m_{ww} = 0$. The second model, Q_{ww}, used $n_{ww} = 7$ and $m_{ww} = 0$ at both state points.

Tables 1 and 2 and Figures 1 and 2 show g_{Cl-O}, $N_O[r]$, and their differences (Δg_{Cl-O} and $\Delta N_O[r]$) at the two state points. The error bars in these figures are bootstrap estimates of the standard deviations due to the limited sample of configurations. The differences between the A model and the two Q models are very small. The values of Δg_{Cl-O} are almost always less than twice their standard deviations, 2σ, while values of $\Delta N_O[r]$ are small, although some are greater than 2σ.

Consider the Q_1 model for g_{Cl-O} first. At 573 K, Δg_{Cl-O} at all r is less than about 2σ, so some of the differences are probably, but not certainly, significant. Table 1 gives values of $N_O^A[r]$ and $\Delta N_O^{Q1}[r]$ at 573 K. The maximum differences between the A and Q_1 model occur at 2.992 and 4.080 Å, where $\Delta N_O^{Q1}[r]$ is 0.11 ± 0.06 and 0.46 ± 0.08, respectively. These are small but significant differences. At 723 K, Δg_{Cl-O} is again mostly less than about 2σ, but some of the differences are significant. Table 2 shows that the maximum differences between models occur at 2.94, 3.36, and 4.34 Å, where $\Delta N_O^{Q1}[r]$ is 0.02 ± 0.01, −0.05 ± 0.02, and 0.09 ± 0.03, respectively. These are extremely small but statistically significant differences.

Figures 3 and 4 give g_{Cl-H}, $N_H[r]$ and their differences (Δg_{Cl-H} and $\Delta N_H[r]$) at the two state points. There are two peaks in g_{Cl-H} corresponding to the two hydrogens in the water molecule. Again, consider first the Q_1 model. The differences between the two models are small. The values of Δg_{Cl-H} are occasionally greater than twice their standard deviations so there are some significant differences. For $\Delta N_H[r]$, there are often significant differences.

At 573 K, there are small shifts in the two peaks in g_{Cl-H} with a slightly deeper minimum between the peaks. For $\Delta N_H[r]$, Table 1 shows that maximum differences between the A and Q_1 models occur at 2.448, 3.536, and 4.896 Å, where $\Delta N_H^{Q1}[r]$ is 0.16 ± 0.09, −0.59 ± 0.10, and 0.21 ± 0.36, respectively. At this state point, our calculation clearly shows the deficiencies of the approximate model.

At 723 K, the shifts in Δg_{Cl-H} are in the opposite direction from those at 573 K. The first peak is shifted away from the Cl^-, whereas the second peak is shifted toward the Cl^-. The minimum between the peaks is not as deep. The shift in the first peak is well outside the 95% confidence interval. The maximum changes in $N_H[r]$ occur near the two peaks, at 2.38 and 3.36 Å, where the changes are −0.09 ± 0.02 and 0.18 ± 0.03, respectively. These changes are small but easily detected by our calculation. The change in $N_H[r]$ persists to 6.1 Å, so the Q_1 model has on average about 0.2 more hydrogen atoms inside 4.9 Å.

Turning to the Q_{ww} model, Figures 1−4 show that Δg and $\Delta N[r]$ are much more uncertain. At 573 K, many of the error bars for the Q_{ww} results overlap the error bars of the Q_1 results,

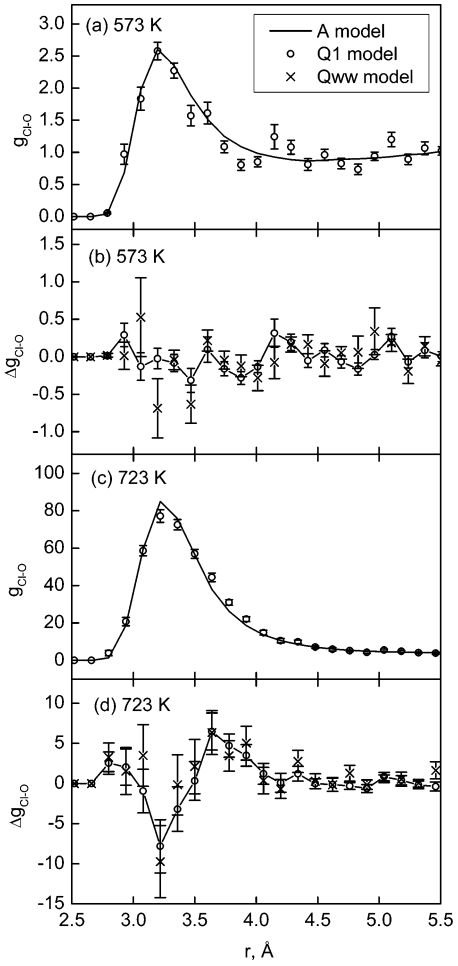

Figure 1. Radial distribution functions (g_{Cl-O}) of chloride ion−water oxygen for A and Q_1 models at 573 K, 0.725 g/cm^3 (panel a) and 723 K, 0.0098 g/cm^3 (panel c). The differences in the functions, Δg_{Cl-O}, between A and Q_1 and A and Q_{ww} are shown for the two state points (panels b and d), respectively.

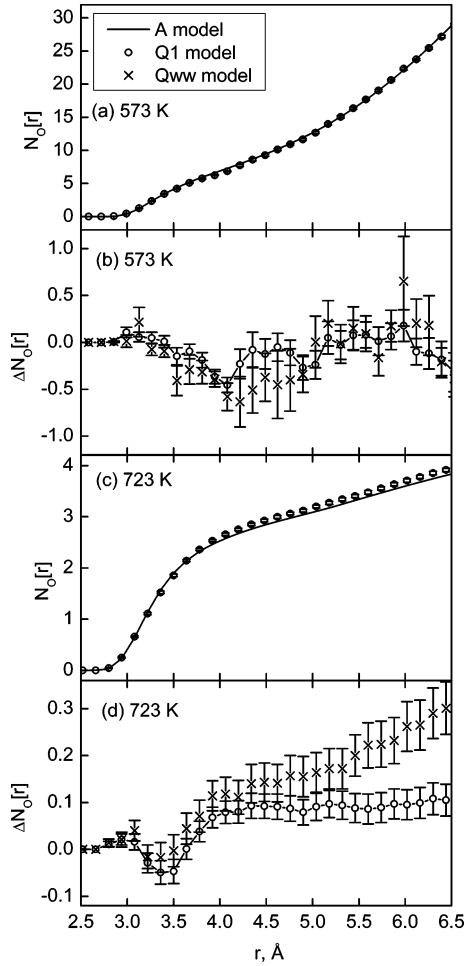

Figure 2. Running coordination number ($N_O[r]$) of water oxygen around the chloride ion for A and Q_1 model at 573 K, 0.725 g/cm^3 (panel a) and 723 K, 0.0098 g/cm^3 (panel c). The differences in the functions, $\Delta N_O[r]$, between A and Q_1 and A and Q_{ww} are shown for the two state points (panels b and d), respectively.

so the differences in Δg and $\Delta N[r]$ are small and could be negligible. At 723 K, Δg for the two quantum models are all within two standard deviations. However, $\Delta N_{Cl-O}[r]$ and $\Delta N_{Cl-H}[r]$ for Q_{ww} has consistently larger values than that for Q_1 beyond about 5.5 Å, indicating that the Q_{ww} model may have 0.2 more waters around Cl^- inside 6.5 Å. However, the two models at short Cl−water distances are still statistically indistinguishable. This indicates that our use of an approximate water model (TIP4P-FQ) does not introduce large errors. When we tried a model with more water−water interactions ($n_{ww} = 30$ and $m_{ww} = 7$), the uncertainties increased substantially with no detectable change in the structure. This increase in uncertainty was predicted by both Pratt and Bukowski independently.[46,47] It occurs because the fluctuations in the energy are proportional to the number of molecules and grow faster than the signal.

3.3. Coordination Numbers. If we define the oxygen coordination number as the number of oxygen atoms with $R_{Cl-O} \leq 4.352$ Å, from Table 1 the average oxygen coordination number at 573 K is 8.67 for the A model, 8.59 ± 0.19 for the Q_1 model, and 8.16 ± 0.24 for the Q_{ww} model. At 723 K, interpolating Table 2 shows that the average oxygen coordination number at 4.352 Å has dropped to 2.76, 2.85 ± 0.03, and 2.90 ± 0.04 for the A, Q_1, and Q_{ww} models, respectively. Similarly, if we define the average hydrogen coordination number as the number of hydrogen atoms inside 2.856 Å, then from Table 1 the average hydrogen coordination numbers at 573 K are 4.65, 4.60 ± 0.08, and 4.21 ± 0.22 for the A, Q_1, and Q_{ww} models, respectively. At 723 K (interpolating Table 2), the average hydrogen coordination numbers have dropped to 2.21, 2.19 ± 0.03, and 2.22 ± 0.04 for the A, Q_1, and Q_{ww} models, respectively.

It is informative to consider the distribution of coordination numbers in addition to the averages. The probability of finding the various coordination numbers was calculated by eqs 8 and 9 and the results are shown in Figure 5 for Cl−O and Cl−H. The distribution of oxygen coordination numbers in Figure 5 varies from 4 to 13 with major contributions from 7, 8, 9, and 10. The distribution is not significantly different for the other models (differences are less than 2σ). The Q_{ww} model again shows larger standard deviations than the Q_1 model. The hydrogen coordination numbers vary from 1 to 7 with major contributions from 4 and 5. This shows that models of these solutions based on only one or two coordination numbers will not be accurate because many different coordination numbers contribute to the solution structure. The fraction of seven-coordinate configurations for O and three-coordinate configurations for H at 573 K may be larger in the Q_{ww} model.

3.4 Structure of Coordinated Water. The average H coordination number at 573 K is almost half of the average O coordination number, showing that almost half of the oxygens in the first oxygen coordination sphere do not have any attached hydrogen atoms in the first hydrogen coordination sphere. This

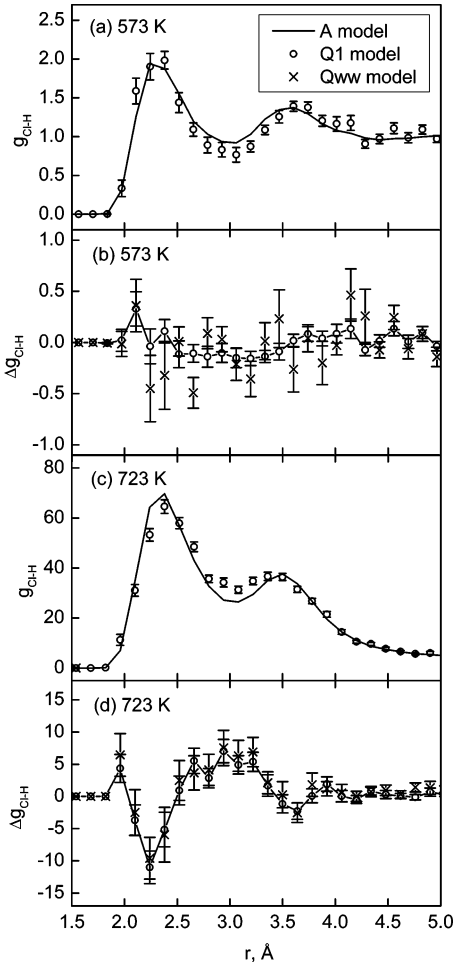

Figure 3. Radial distribution functions (g_{Cl-H}) of chloride ion−water hydrogen for A and Q_1 model at 573 K, 0.725 g/cm^3 (panel a) and 723 K, 0.0098 g/cm^3 (panel c). The differences in the functions, Δg_{Cl-H}, between A and Q_1 and A and Q_{ww} are shown for the two state points (panels b and d), respectively.

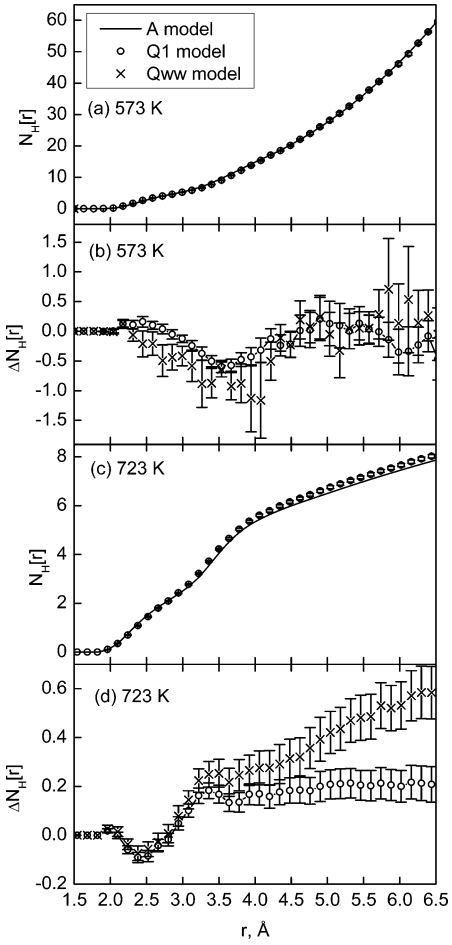

Figure 4. Running coordination number ($N_H[r]$) of water hydrogen around the chloride ion for A and Q_1 model at 573 K, 0.725 g/cm^3 (panel a) and 723 K, 0.0098 g/cm^3 (panel c). The differences in the functions, $\Delta N_H[r]$, between A and Q_1 and A and Q_{ww} are shown for the two state points (panels b and d), respectively.

indicates that there may be many different orientations of water in the solvation structure around the chloride ion. To explore this further, we define a coordinated water as one that has its oxygen in the first oxygen coordination sphere, $R_{Cl-O} < 4.532$ Å. Then we categorize H−Cl distances in these coordinated waters as either short ($R_{Cl-H} \leq 2.856$ Å), medium ($R_{Cl-H} > 2.856$ Å and $R_{Cl-H} < R_{Cl-O}$), or long ($R_{Cl-H} \geq R_{Cl-O}$). Thus, short hydrogens are hydrogens that are in the first hydrogen coordination sphere of Cl^-. With these definitions, we classified all water molecules in the first coordination sphere ($R_{Cl-O} < 4.352$ Å) into six categories (SS, MM, LL, SM, SL, and ML), where for example, SM denotes a water molecule with one short and one medium H−Cl distance. Thus, SS denotes a water with two short hydrogen bonds, so it is essentially a bifurcated hydrogen bond, while SL denotes a single strong hydrogen bond with the second hydrogen pointing away from the chloride ion.

Figures 6 and 7 show plots of the distribution of the ab initio pairwise interaction energy between each water and the chloride ion ($U^Q_{Clw,pair}$) as a function of R_{Cl-O} for all water molecules in the first coordination sphere. These plots are for configurations from the A model. Plots for the Q models are the same, but the weights of the points are not equal. The weights seem to be randomly distributed, so the qualitative conclusions are the same for all the models. Our 500 configurations were used to calculate the relative populations of the various water structures. Table 3 gives the resulting relative populations of the different categories of structures in the first coordination sphere of the A and Q_1 models. The differences between the models are small, so we will only discuss the Q_1 model, but the discussion also applies to the A model. As expected, there are fewer coordinated waters at the low-density state point (723 K, 0.0098 g/cm^3). We will show that the difference in structure can largely be attributed to the absence of the less strongly bound waters at lower density.

At both state points, the most common structure for these first-shell water molecules is SL; that is, the water has a single strong hydrogen bond with the chloride ion and the other hydrogen points away from the ion. On average, 45.6% and 56.9% of the waters in the first coordination sphere have this structure at 573 and 723 K, respectively. These waters are mainly responsible for the two peaks that are seen in g_{Cl-H}. As seen in Figures 6 and 7, they are also, on average, the most strongly bound waters. At any given R_{Cl-O}, the structure with the lowest possible energy has this orientation (though it is classified as ML when $R_{Cl-O} \geq 3.7$ Å). The dashed line in Figures 6 and 7 shows this minimum energy. The global minimum in pair interaction energy occurs at an R_{Cl-O} near 3.15 Å, and a considerable number of SL waters have an R_{Cl-O} less than this distance. Presumably, these waters are being pushed close to the Cl^- by other molecules or by thermal fluctuations.

The next most common structure is ML, with one H pointing toward (but not close to) the Cl^- and the other pointing away. On average, 31.4% and 13.6% of the coordinated waters are

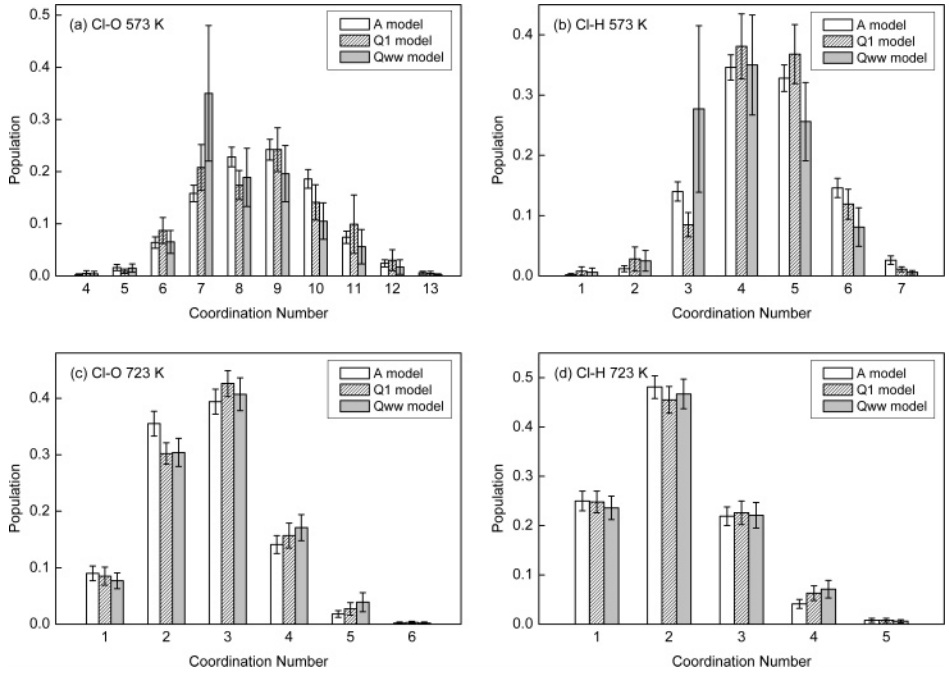

Figure 5. Distributions of coordination numbers of water oxygen and hydrogen around the chloride ion for A, Q_1, and Q_{ww} models at 573 K, 0.725 g/cm^3 and 723 K, 0.0098 g/cm^3.

ML waters at 573 and at 723 K, respectively. A significant number (but less than half) of these waters have positive energies of pairwise interaction with the Cl^- ion, $U^Q_{Clw,pair}$, at 573 K. At 723 K, very few have positive $U^Q_{Clw,pair}$. Presumably, the waters with positive $U^Q_{Clw,pair}$ are strongly bound to other waters. They must occur less frequently at low density.

Most of the remaining structures have fairly low populations. The third most common structure, MM, has two H's pointing toward the Cl^-, but they are not close. At 573 K, 12.6% of the waters are MM, and at 723 K, 14.3% are MM. The R_{Cl-O} distance tends to be long in these structures, and the energies are on average lower than that of the ML waters. However, for $R_{Cl-O} < 3.7$ Å, other orientations are always lower in energy. The next most common structure, SM, has both H's pointing toward the Cl^- with one short bond. There are few of these molecules, and their energies are generally low but not the lowest possible. At 573 K, 5.5% of the waters are SM, while at 723 K, 12.7% are SM. The average R_{Cl-O} is similar but slightly larger than for the SL configuration. The SS configuration is a bifurcated H bond. There are very few of these at either state point. Their energies are all low, but again, not the lowest possible. At 573 K, 0.7% of the waters are SS, while at 723 K, 2.4% are SS. Their R_{Cl-O} is uniformly short and normally less than 3.15 Å (the radius at the global energy minimum). The LL configuration has both of the H's pointing away from the Cl^- ion. On average, 4.2% of the waters are LL at 573 K and 0.10% at 723 K. This rare structure always has positive $U^Q_{Clw,pair}$ and its R_{Cl-O} is mostly long. Presumably, these waters are strongly interacting with other waters either in the first or second hydration shell.

One expects that, as the density is lowered from 0.725 to 0.0098 g/cm^3 and the temperature is raised, the less strongly bound waters are more likely to leave. This expectation is confirmed by two features of Figures 6 and 7 and Table 3, which show that the SL, SM, and SS structures have a low R_{Cl-O} and a low $U^Q_{Clw,pair}$, and these low energy structures are more probable at 723 K. The ML and LL structures have high R_{Cl-O} and a high $U^Q_{Clw,pair}$ and, as expected, these are less probable at 723 K. The MM structure is an intermediate case. A comparison of the same structure in Figures 6 and 7 indicates a smaller fraction of high $U^Q_{Clw,pair}$ at 723 K for all structures.

At 723 K and 0.0098 g/cm^3, there are many configurations with an oxygen coordination number of two. The lowest energy configuration for $Cl(H_2O)_2$ in the gas phase has a O−Cl−O angle of 56.9°, with the two waters hydrogen bonded to each other. Clusters with more water often have global minima with the Cl^- at the edge of the cluster (surface state).[18,27,28,42] There is also a local minimum for $Cl(H_2O)_2$ with the O−Cl−O angle equal to 180°, but it is 9 kJ/mol higher in energy than the global minimum. We have explored the distribution of O−Cl−O angles in configurations with coordination number two at 723 °C. Figure 8 gives a plot of the fraction of molecules in equally spaced bins (12° wide) for the A and Q_1 models. Figure 8 also shows the probability for random placement of the oxygens on a sphere. Very low angles (<48°) are very rare, presumably because of the expected steric repulsion between the oxygens. Given the error bars, it is difficult to see a preference for any angles above 48°. Certainly, there is no detectable preference either for angles near the global minimum at 56.9° or near the local minimum at 180°. Possible reasons for this lack of preference are that (1) the temperature is too high, so that many states with larger O−Cl−O angles are accessible, and (2) second-shell waters participate in hydrogen bonding with the two first-shell waters, thus stabilizing larger angles. It is clear that, at 723 K and 0.0098 g/cm^3, minimum energy structures are not a useful guide to the structures actually present.

4. Discussion

4.1. Comparison with Experimental Results. There are no quantitative comparisons with experimental results because of differences in temperature and pressure. In addition, experimental results are usually for concentrated solutions (1 mol/kg or more), where ion pairing affects the coordination numbers (see Chialvo and Simonson[15] for a clear demonstration). Nevertheless, Table 4 shows that the radius at first maximum (R_{max}) in the distribution functions and coordination numbers

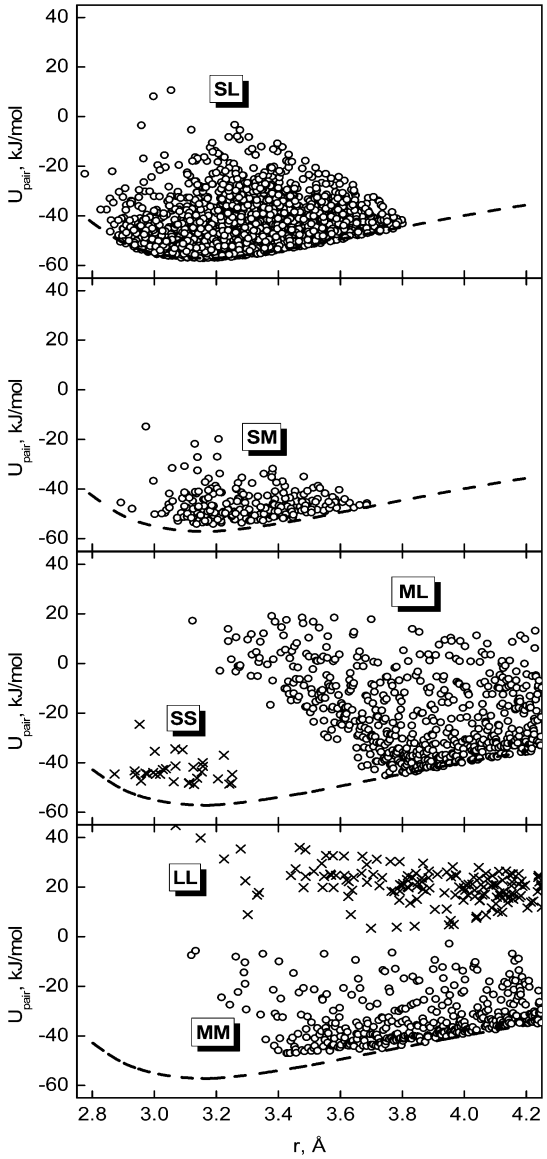

Figure 6. Distribution of the quantum pairwise interaction energy between the water and the chloride ion ($U^{Q}_{Clw,pair}$) vs the distance between Cl^- and water oxygen, R_{Cl-O}, for all water molecules in the first coordination sphere at 573 K, 0.725 g/cm^3. The definitions of SL, SM, etc. are given in Section 3.4. The dashed line is the lowest possible energy (U_{pair}) as a function of R_{Cl-O}. The symbols are: third panel, × is SS, ○ is ML; fourth panel, × is LL, ○ is MM.

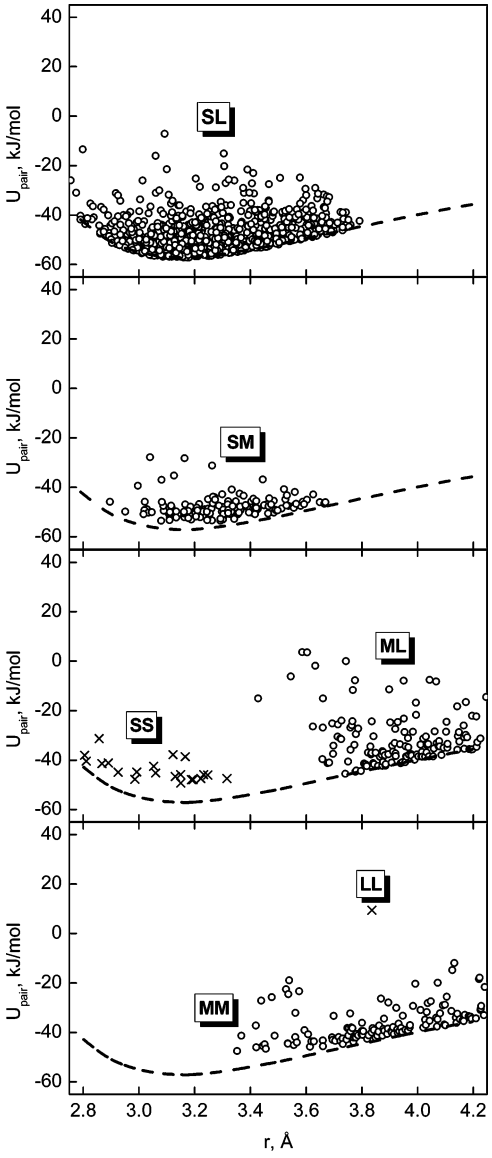

Figure 7. Distribution of the quantum pairwise interaction energy between the water and the chloride ion ($U^{Q}_{Clw,pair}$) vs the distance between Cl^- and water oxygen, R_{Cl-O}, for all water molecules in the first coordination sphere at 723 K, 0.0098 g/cm^3. The definitions of SL, SM, etc. are given in Section 3.4. The dashed line is the lowest possible energy (U_{pair}) as a function of R_{Cl-O}. The symbols are the same as Figure 6.

(CN) are in qualitative agreement with recent experimental results at high temperatures. The results of neutron diffraction experiments with isotopic substitution (NDIS) on $NiCl_2$ solutions by Enderby[49] and de Jong et al.[50] show that R_{max} increases with temperature at high density and the coordination numbers of hydrogen and oxygen decrease. The results of Yamaguchi et al. for the hydrogen coordination number using Gaussian fits to the peaks in g_2 are lower than the other experimental results at high temperatures.[51] Yamaguchi and Soper reported NDIS experiments on 8.6 and 3 mol/kg LiCl solutions at 470 and 648 K, respectively.[52] They analyzed their results using an empirical potential structure refinement (EPSR) to derive the chlorine−oxygen and chlorine−deuterium radial distribution functions. They did not know whether Li−Cl ion pairing had partly occurred, and the temperatures were not the same as ours. However, Table 4 shows that their high-temperature results are in qualitative agreement with the present studies. Yamaguchi and Soper concluded that there was a shell of orientationally uncorrelated water molecules at high temperatures, and some of the waters did not have their OD bonds oriented toward the chloride ion.[51] This is now confirmed by the present study, and we are able to give quantitative estimates of the number of water molecules with each of six different structures. Also, we have calculated not only the average coordination number but also the frequency with which the various coordination numbers occur. The estimated uncertainties in the coordination numbers of the present results are lower than any of the estimated experimental uncertainties.

4.2. Comparison with Simulations. There are a large number of structure determinations from simulations of aqueous chloride models at ambient conditions[15,21−24,48] and a few at high temperatures.[13,14,53−59] Most of the qualitative features of the results of previous simulations are in agreement with one another. We tentatively conclude that these features are also true of real aqueous Cl^- solutions. For instance, the coordination

TABLE 3: Average Relative Frequencies (in %) of Occurrence of the Various Kinds of Water in the First Coordination Sphere of Cl^- at the Two State Points for the A and Q_1 Models[a]

	573 K 0.725 g/cm^3		723 K 0.0098 g/cm^3	
structure	A	Q_1	A	Q_1
SS	0.7(1)[b]	0.7(2)	1.6(3)	2.4(6)
MM	13.3(5)	12.6(10)	12.1(9)	14.3(11)
LL	4.8(3)	4.2(7)	0.10(8)	0.10(5)
SM	5.6(4)	5.5(9)	10.6(9)	12.7(12)
SL	45.5(7)	45.6(14)	62.4(13)	56.9(15)
ML	30.1(6)	31.4(16)	13.1(9)	13.6(11)

[a] These are the % of water molecules with the given structure. The total average numbers of water in the first coordination sphere are 8.67 and 2.76 for the A model at 573 and 723 K respectively, and 8.58 (21) and 2.86(5) for the Q_1 model at the two temperatures. [b] The number in parentheses is the standard deviation of the last digit(s) estimated by bootstrap resampling.

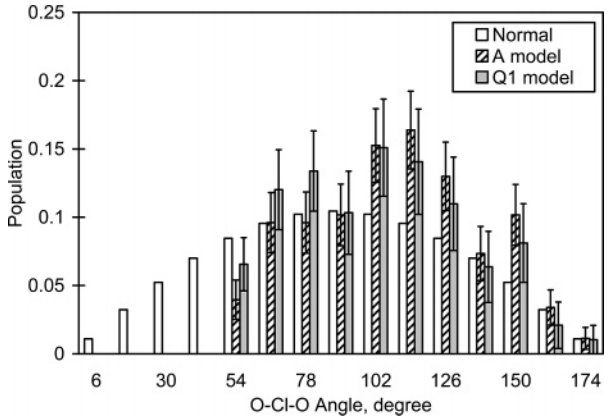

Figure 8. Histogram of the probable occurrence of O−Cl−O angles in configurations with coordination number 2 at 723 K and 0.0098 g/cm^3. Normal represents the probability for random placement of the oxygens on a sphere around the chlorine atom, while the A model and Q1 model are defined in the text.

numbers decrease with increasing temperature and decreasing density.

Several simulation studies indicate the hydration sphere of Cl^- is disordered, in agreement with experiments and the present study. Tongraar and Rode concluded that, at ambient conditions, there exists "a combination of linear and bridged forms, together with a competition between solvation of the ion and hydrogen bonding among the water molecules."[23] Öhrn and Karlström found that the waters in the first shell of Cl^- were "more randomly positioned relative to each other" than they are in aqueous Na^+.[22] However, Heuft and Meijer's DFT simulation[21] with 64 waters found oxygen and hydrogen coordination numbers of 5.8 and 5.2, respectively, indicating little disorder. Their oxygen coordination number is in poor agreement with the experimental value of 10.8 at 298 K.[47]

Tongraar and Rode have reviewed the oxygen coordination numbers at ambient conditions from the literature, which vary from 5.1 to 8.4.[23] Recently, Chialvo and Simonson found a coordination number of 7.4 for oxygen and 7.2 for hydrogen, indicating that essentially all of the oxygens are hydrogen bonded to the Cl^-.[15] It is very difficult to say which of these discordant results is the most accurate. However, at 673−683 K, where comparisons are also possible, there is less disagreement among the prior simulations.[13,14,55−58] For instance, the oxygen coordination number varies relatively slowly (plateau) from 7.5 ± 0.5 at 0.2 g/cm^3 to 8.25 ± 0.3 at 0.6 g/cm^3 at 673 K. In this region, the CN is also relatively insensitive to model differences and temperature changes at constant density.[55,57] Assuming a negligible temperature coefficient, these results are consistent with the present result at 573 K, $N_O[R_{cut}]$. Similarly, our result at 723 K is consistent with an extrapolation of the results of Kubo et al. at 0.05 g/cm^3.[14] Thus we conclude that, as expected, the present results are in qualitative agreement with both the previous experiments and simulations.

Indeed, it appears that the structural properties of these solutions are less sensitive to the model than the free energy. This is illustrated by the fact that the structural differences between the A and Q_1 models are small, while the free energy differences are significant. However, by using the Q_1 and Q_{ww} models to test the structural predictions of the A model, the present results are more reliable than those from any model potential. We also believe and that any differences between our model and "real aqueous Cl^-" are small. The discussion of uncertainties below gives our reasons for this belief.

TABLE 4: Experimental Results at High Densities Compared to the Present Results at 573 K

T/K	298.15	298.15	298.15	350	373	470	573	573	648	648
P/MPa	0.1	0.1	psat	psat	100	1.4	100	14.7	169	169
d/gcm^{-3}[a]	0.997	0.997	0.997	0.974	1.068	0.868	1.048	0.725	0.795	0.795
method[b]	NDIS	NDIS	EPSR	EPSR	NDIS	EPSR	NDIS	ABC /FEP	NDIS	EPSR
molality	2	3	9.5	8.6	2	8.6	2		3	3
salt	$NiCl_2$	LiCl	LiCl	LiC1	$NiCl_2$	LiCl	$NiCl_2$		LiCl	LiCl
$R_{H\,max}$[c]	2.28(3)	2.23(2)	2.27		2.30(3)		2.39(4)	2.3	2.33(2)	2.4
$R_{H\,cut}$[d]		Gauss[d]	2.95	2.95	2.8	2.95	2.8	2.856[f] 2.80	Gauss	2.95
$N_H[R_{cut}]$[e]	6.4(3)	5.8(2)	4.9(2)	5.5(2)	6.9(5)	5.2(2)	4.9(5)	4.60(8) 4.35(8)	2.5(2)	3.8(3)
$R_{O\,max}$[c]	3.1(1)		3.16		3.3(2)		3.4(2)	3.2		3.2
$R_{O\,cut}$[d]			4.50	4.50		4.50		4.352[f] 4.50		4.50
$N_O[R_{cut}]$			10.8(3)	10.8(3)		9.9(3)		8.6(2) 9.4(2)		9.5(5)
reference	49	51	52	52	50	52	50	present work	51	52

[a] Density, d, of pure water at the experimental temperature, T, and pressure, P. [b] NDIS is neutron diffraction with isotopic substitution. EPSR is NDIS with an empirical potential structure refinement. ABC/FEP is the present calculation. [c] $R_{H\,max}$ and $R_{O\,max}$ indicate the distance to the first maximum in g_{Cl-H} and g_{Cl-O}. [d] R_{cut} is cut off distance for N_H and N_O (see eq 8). Gauss means that the coordination number was established by fitting the peak to a Gaussian. [e] $N_H[R_{cut}]$ and $N_O[R_{cut}]$ are the coordination numbers (see eq 8). [f] In addition to the R_{cut} determined from our model, a second value of R_{cut} and the corresponding $N[R_{cut}]$ is given to facilitate comparison with the experimental results.

4.3. Estimation of Uncertainties. The aim of the present effort was to calculate the structure of a model with: (1) all pairwise solute−water interactions calculated by MP2/aug-cc-pVDZ, (2) all solute−water multibody interactions calculated with DFT/B3LYP/aug-cc-pVDZ, and (3) all water−water interactions calculated with the TIP4P-FQ model. We have reported uncertainties (calculated by bootstrap resampling[45]) of our results due to using a limited sample of independent configurations. These uncertainties were found to be small in the present calculations, indicating that the A model is accurate enough to adequately sample the configurations of the Q_1 model, and as a consequence, the inaccuracy of the approximate model is not affecting the result.

Here we discuss estimates of other sources of uncertainty. First, our calculation only uses quantum pairwise interactions between the nearest *n* molecules and multibody interactions between the nearest *m* molecules. Uncertainties due to this limited sampling are estimated by varying the values of *n* and *m* and extrapolating to $n = \infty$ (if necessary). Although we used $n_{Clw} = 60$ in our calculations of structure at 573 K, the contributions of the outer 45 water molecules to Δg_{Cl-O} and Δg_{Cl-H} are negligible, showing that these outer water molecules have little effect on the structure of the first solvation shell. In calculating $\Delta_h G(A \rightarrow Q)$, extrapolation to $n = \infty$ makes a small contribution at 573 K. However at 723 K, $n = 15$ is sufficient for $\Delta_h G(A \rightarrow Q)$, Δg, and ΔN.

In our calculations of $\Delta_h G(A \rightarrow Q)$, the main uncertainty is in the accuracy of the quantum method. This uncertainty can be estimated by doing calculations with more accurate quantum methods and larger basis sets or from prior experience with the quantum methods and basis sets. In the calculations of $\Delta_h G(A \rightarrow Q)$, we have previously estimated the uncertainty of the quantum method as 5 kJ/mol, and two checks against experimental data indicate this estimate is about right.[3,4] In the present calculations of Δg and ΔN, we do not have good estimates of their uncertainty due to the quantum method because we have limited previous experience with these quantities, and calculations with a larger basis set or better method were beyond our means. However, from studies of a chloride ion with one water, Xantheas concluded that "The MP2/aug-cc-pVDZ level of theory consists of a reasonable compromise between feasibility and accuracy since it yields bond lengths and energetics within <0.04 Å and <3 kJ/mol from the MP4/aug-cc-pVTZ results, respectively".[48] Xantheas's results were particularly insensitive to the level of theory (MP2 versus MP4). Compared with the free energy, the structural results are less sensitive to the model, as shown by the small differences between the A and Q models in Figures 1−5.

In principle, the uncertainty due to the approximate model for the water−water interactions can be estimated by including the quantum water−water interaction energies in the calculation of structure. However, as seen above, this method is not satisfactory because of the increase in uncertainties when water−water interaction energies are added in. A better way to estimate these uncertainties would be to repeat the calculations with a much better approximate model for the water−water interactions energies.

In our model, the motion of the nuclei is classical, not quantum mechanical, so that the structural properties do not have the slight decrease in the maxima, increase in the minima, and shift of the peaks to larger *r* than would be expected if the quantum motion of the nuclei were taken into account.[60−62] One method of estimating this effect, which is most important for the hydrogen nuclei, would be to add path integral methods for the hydrogen motion to a classical simulation and see how much this changes the radial distribution function of the classical model.

A calculation of the structure of aqueous chloride ion without the above approximations is entirely feasible but unfortunately beyond the scope of the present paper. However, we do have the structure of a high-level quantum model, and we expect that calculations without the above approximations will not be much different from our results.

Acknowledgment. This research was supported by the Chemical Sciences, Geosciences, and Biosciences Division, Office of Basic Energy Science, Office of Science, U.S. Department of Energy, under grant no. DEFG02-89ER-14080. We also acknowledge the computer facilities of the University of Delaware, including facilities made available by an NSF Major Research Instrumentation Program (grant no. CTS-9724404).

References and Notes

(1) Wood, R. H.; Yezdimer, E. M.; Sakane, S.; Barriocanal, J. A.; Doren, D. J. *J. Chem. Phys.* **1999**, *110*, 1329.
(2) Sakane, S.; Yezdimer, E. M.; Liu, W.; Barriocanal, J. A.; Doren, D. J.; Wood, R. H. *J. Chem. Phys.* **2000**, *113*, 2583.
(3) Liu, W.; Sakane, S.; Wood, R. H.; Doren, D. J. *J. Phys. Chem. A* **2002**, *106*, 1409.
(4) Liu, W.; Wood, R. H.; Doren, D. J. *J. Phys. Chem. B* **2003**, *107*, 9505.
(5) Wood, R. H.; Liu, W.; Doren, D. J. *J. Phys. Chem. A* **2002**, *106*, 6689.
(6) Liu, W.; Wood, R. H.; Doren, D. J. *J. Chem. Phys.* **2003**, *118*, 2837.
(7) Galobardes, J. F.; van Hare, D. R.; Rogers, L. B. *J. Chem. Eng. Data* **1981**, *26*, 363.
(8) Conway, B. E. *Chem. Soc. Rev.* **1992**, 253.
(9) Markovits, G. Y.; Choppin, G. R. *Ion Exchange and Solvent Extraction*; Marcel Dekker: New York, 1973.
(10) Brodholt, J.; Wood, B. J. *Geophys. Res.* **1993**, *98*, 519.
(11) Ohtaki, H.; Radnai, T. *Chem. Rev.* **1993**, *93*, 1157.
(12) Patra, M.; Karttunen, M. *J. Comput. Chem.* **2004**, *25*, 678.
(13) Konishan, S.; Rasaiah, J. C.; Dang, L. X. *J. Chem. Phys.* **2001**, *114*, 7544.
(14) Kubo, M.; Levy, R. M.; Rossky, P. J.; Matubayasi, N.; Nakahara, M. *J. Phys. Chem.* **2002**, *106*, 3979.
(15) Chialvo, A. A.; Simonson, J. M. *J. Chem. Phys.* **2003**, *119*, 8052; **2006**, *124*, 154509.
(16) Seminario, J. M. in *Molecular Dynamics from Classical to Quantum Methods*; Balbuena, P. B., Seminario, J. M., Eds.; Elsevier: Amsterdam, 1999; Chapter 6.
(17) Jungwirth, P.; Tobias, D. J. *J. Phys. Chem. A* **2002**, *106*, 379.
(18) Tobias, D. J.; Jungwirth, P.; Parinello, M. *J. Chem. Phys.* **2001**, *114*, 7036.
(19) Schlegel, H. B.; Millam, J. M.; Iyengar, S. S.; Voth, G. A.; Daniels, A. D.; Scuseria, G. A.; Frisch, M. J. *J. Chem. Phys.* **2001**, *114*, 9758.
(20) Schlegel, H. B.; Iyengar, S. S.; Li, X.; Millam, J. M.; Voth, G. A.; Daniels, A. D.; Scuseria, G. A.; Frisch, M. J. *J. Chem. Phys.* **2002**, *117*, 9758.
(21) Heuft, J. M.; Meijer, E. J. *J. Chem. Phys.* **2003**, *119*, 11788.
(22) Öhrn, A.; Karlström, G. *J. Phys. Chem. B* **2004**, *108*, 8452.
(23) Tongraar, A.; Rode, B. M. *Phys. Chem. Chem. Phys.* **2003**, *5*, 357. Table 2 gives a list of earlier results at ambient conditions.
(24) Tongraar, A.; Rode, B. M. *Chem. Phys. Lett.* **2005**, *403*, 314.
(25) Tongraar, A.; Liedl, K. R.; Rode, B. M. *J. Phys. Chem. A* **1998**, *102*, 10340.
(26) Shoeib, T.; Ruggiero, G. D.; Siu, K. W. M.; Hopkinson, A. C.; Williams, I. H. *J. Chem. Phys.* **2002**, *117*, 2762.
(27) Merrill, G. N.; Webb, S. P. *J. Phys. Chem. A* **2003**, *107*, 7852.
(28) Kemp, D. D.; Gordon, M. S. *J. Phys. Chem. A* **2005**, *109*, 7688.
(29) Dupuis, M.; Schenter, G. K.; Garrett, B. G.; Arcia, E. E. *J. Mol. Struct. (THEOCHEM)* **2003**, *632*, 173.
(30) Wesolowski, T.; Warshel, A. *J. Phys. Chem.* **1994**, *98*, 5183.
(31) Wesolowski, T.; Muller, R. P.; Warshel, A. *J. Phys. Chem.* **1996**, *100*, 15444.
(32) Akhmatskaya, E. V.; Cooper, M. D.; Burton, N. A.; Masters, A. J.; Hillier, I. H. *Chem. Phys. Lett.* **1997**, *267*, 105.
(33) Vaidehi, N.; Wesolowski, T. A.; Warshel, A. *J. Chem. Phys.* **1997**, *97*, 4264.

(34) Bentzien, J.; Muller, R. P.; Florian, J.; Warshel, A. *J. Phys. Chem. B* **1998**, *102*, 2293.
(35) Vaughn, S. J.; Akhmatskaya, E. V.; Vincent, M. A.; Masters, A. J.; Hillier, I. H. *J. Chem. Phys.* **1999**, *110*, 4338.
(36) Strajbl, M.; Hong, G.; Warshel, A. *J. Phys. Chem. B* **2002**, *106*, 13333.
(37) Murdock, S. E.; Lynden-Bell, R. M.; Kohanoff, J.; Sexton, G. J. *Phys. Chem. Chem. Phys.* **2002**, *4*, 3016.
(38) Torrie, G. M.; Valleau, J. P. *Chem. Phys. Lett.* **1974**, *28*, 578.
(39) Torrie, G. M.; Valleau, J. P. *J. Comput. Phys.* **1977**, *23*, 187.
(40) Mielke, S. L.; Garrett, B. C.; Peterson, K. A. *J. Chem. Phys.* **1999**, *111*, 3806.
(41) Forester, T. R.; Smith, W. *DL-POLY*; Daresbury Laboratory: Daresbury, U.K., 1995.
(42) Rick, S. W.; Stuart, S. J.; Berne, B. J. *J. Chem. Phys.* **1994**, *101*, 6141.
(43) Frisch, M. J.; Trucks, G. W.; Schlegel, H. B.; Scuseria, G. E.; Robb, M. A.; Cheeseman, J. R.; Montgomery, J. A., Jr.; Vreven, T.; Kudin, K. N.; Burant, J. C.; Millam, J. M.; Iyengar, S. S.; Tomasi, J.; Barone, V.; Mennucci, B.; Cossi, M.; Scalmani, G.; Rega, N.; Petersson, G. A.; Nakatsuji, H.; Hada, M.; Ehara, M.; Toyota, K.; Fukuda, R.; Hasegawa, J.; Ishida, M.; Nakajima, T.; Honda, Y.; Kitao, O.; Nakai, H.; Klene, M.; Li, X.; Knox, J. E.; Hratchian, H. P.; Cross, J. B.; Bakken, V.; Adamo, C.; Jaramillo, J.; Gomperts, R.; Stratmann, R. E.; Yazyev, O.; Austin, A. J.; Cammi, R.; Pomelli, C.; Ochterski, J. W.; Ayala, P. Y.; Morokuma, K.; Voth, G. A.; Salvador, P.; Dannenberg, J. J.; Zakrzewski, V. G.; Dapprich, S.; Daniels, A. D.; Strain, M. C.; Farkas, O.; Malick, D. K.; Rabuck, A. D.; Raghavachari, K.; Foresman, J. B.; Ortiz, J. V.; Cui, Q.; Baboul, A. G.; Clifford, S.; Cioslowski, J.; Stefanov, B. B.; Liu, G.; Liashenko, A.; Piskorz, P.; Komaromi, I.; Martin, R. L.; Fox, D. J.; Keith, T.; Al-Laham, M. A.; Peng, C. Y.; Nanayakkara, A.; Challacombe, M.; Gill, P. M. W.; Johnson, B.; Chen, W.; Wong, M. W.; Gonzalez, C.; Pople, J. A. *Gaussian 03*, revision C.02; Gaussian, Inc.: Wallingford, CT, 2004.
(44) Boys, S. F.; Bernardi, F. *Mol. Phys.* **1970**, *19*, 553.
(45) Efron, B. *The Jackknife, the Bootstrap and Other Resampling Plans*; Regional Conference Series in Applied Mathematics;Society for Industrial and Applied Mathematics: Philadelphia, PA, 1982.
(46) Pratt, L. R. Private communication; see also Los Alamos Technical Report LA-UR-05-0873.
(47) Bukowski, R. Private communication.
(48) Xantheas, S. S. *J. Phys. Chem.* **1996**, *100*, 9703.
(49) Enderby, J. E. *Chem. Soc. Rev.* **1995**, 159.
(50) de Jong, P. H. K.; Neilson, G. W.; Bellissent-Funel, M. C. *J. Chem. Phys.* **1996**, *105*, 5155.
(51) Yamaguchi, T.; Yamagami, M.; Ohzono, H.; Wakita, H.; Yamanaka, K. *Chem. Phys. Lett.* **1996**, *252*, 317.
(52) Yamaguchi, T.; Soper, A. K. *J. Chem. Phys.* **1999**, *110*, 3529.
(53) For a review of earlier literature on aqueous Cl^- ion, see Floris, F. M.; Tani, A. In *Molecular Dynamics: From Classical to Quantum Methods*; Balbuena, P. B., Seminario, J. M., Eds.; Elsevier: Amsterdam, 1999; Chapter 10, Section 6, pp 405−412.
(54) Cummings, P. T.; Cochran, H. D.; Simonsen, J. M.; Mesmer, R. E.; Karaborni, S. *J. Chem. Phys.* **1991**, *94*, 5606.
(55) Balbuena, P. B.; Johnston, K. P.; Rossky, P. J. *J. Phys. Chem.* **1996**, *100*, 2706.
(56) Lee, S. H.; Cummings, P. T.; Simonson, J. M.; Mesmer, R. E. *Chem. Phys. Lett.* **1998**, *293*, 289.
(57) Chialvo, A. A.; Cummings, P. T.; Simonson, J. M.; Mesmer, R. E. *J. Chem. Phys.* **1999**, *110*, 1064.
(58) Rasaiah, J. C.; Noworyta, J. P.; Koneshan, S. *J. Am. Chem. Soc.* **2000**, *122*, 11182.
(59) Noworyta, J. P.; Koneshan, S.; Rasaiah, J. C. *J. Am. Chem. Soc.* **2000**, *122*, 11194.
(60) Kuharski, R. A.; Rossky, P. J. *J. Chem. Phys.* **1985**, *82*, 5164.
(61) DelBuono, G. S.; Rossky, P. J.; Schnitker, J. *J. Chem. Phys.* **1991**, *95*, 728.
(62) Gai, H.; Dang, L. X.; Schenter, G. K.; Garrett, B. C. *J. Phys. Chem.* **1995**, *99*, 13303.